NEW DEVELOPMENTS ON SLAG MODELLING AT ARCELORMITTAL MAIZIÈRES

Jean Lehmann, Nicolas Bontems, Marie Simonnet & Pascal Gardin
ArcelorMittal Maizières Research S.A., France

Ling Zhang
CSIRO Minerals, Australia

ABSTRACT

Recent developments on slag modeling at ArcelorMittal Maizières have two aspects: (i) the improvement of the so-called Cell model for metallurgical slags by an improved description of the existing short range ordering and (ii) the use of the Cell model in coupled computer codes. The improvement of the Cell model for metallurgical slags is expected to come from the development of the Generalized Central Atom model which provides a description of the close vicinity of all atoms in the solution. The same formalism is already used for liquid steel and gives promising results in particular for highly concentrated solutions. On the other side, the slag model is used through our home-built chemical equilibrium code CEQCSI as a component of complex models combining thermodynamics and kinetics and/or fluid mechanics. The first example is a precipitation model based on the classical nucleation/growth theory which can be applied to complex liquid-oxide inclusions but also to complex solid precipitates. A DQMOM method has been recently implemented in this model which drastically shortens computing times and, as a consequence, opens new prospects for its potential applications. A second example is given by the coupling with Fluent™ to combine local chemical equilibrium calculations with fluid dynamics in order to describe complex metallurgical reactors. An example of development of such a model is the description of desulfurization operations in secondary metallurgy vessels.

INTRODUCTION

Understanding and then controlling complex industrial processes as those nowadays in operation in ArcelorMittal steelmaking shops require the development of sophisticated models that more and more combine contributions of several scientific areas such as thermodynamics, chemical kinetics and fluid dynamics.

ArcelorMittal Maizières R&D is largely involved in such an approach with sustained actions in each of these domains taken separately as well as in the construction of combined complex models. In thermodynamics, the development of the General Central Atom model for liquid steel and metallurgical slags started a few years ago and shows good prospects for highly alloyed steels. For slags, it is an extension of the so-called Cell model and it is currently developed in collaboration with CSIRO. In kinetics, the main effort consists in improving the model initially developed for the precipitation of liquid oxides making it more efficient in terms of computing times by using the DQMOM method which is a recent mathematical technique used to solve the population balance equation (PBE). Finally, thermodynamics, and in the near future kinetics, is combined with fluid dynamics to describe metallurgical reactions occurring in steelmaking vessels such as desulfurization in ladle.

THERMODYNAMICS: THE GENERALIZED CENTRAL ATOM MODEL

The Cell Model proposed by Gaye *et al.* [1] was one of the first comprehensive models (if not the first!) for complex metallurgical slags. It is based on the quasichemical approach [2] and offers a description of the neighborhood of the oxygen anions in terms of their closest cations. It has then been extended to other anions than oxygen: sulfur and fluorine [3, 4, 5]. It is now available for slags compositions belonging to the system SiO_2-TiO_2-$Ti2O_3$-Cr_2O_3-Al_2O_3-Fe_2O_3-CrO-FeO-MgO-MnO-CaO and containing up to 10-20 %CaF_2 and a few percents of sulfur. More recently, an extension to the oxi-sulfides has been proposed [6] and validated on the system SiO_2-Al_2O_3-Fe_2O_3-FeO-MgO-MnO-CaO-S. This work already showed the necessity of a more detailed description of the existing short range ordering (SRO) since obtaining a satisfactory representation for these oxi-sulfides required to consider as neighbors of each anion not only the nearest cations but also the nearest anions.

The recent development in terms of thermodynamic modeling at ArcelorMittal Maizières results from a desire to improve the Cell Model particularly for high silica slags and also to have a model able to describe high alloyed and highly segregated liquid steels. Indeed, for highly alloyed liquid steel, we initially chose to develop the Central Atom model approach originally proposed by Lupis and Elliott [7] and very similar to the *surrounded atoms model* developed at about the same period at the LTPCM [8, 9]. But, despite its merits, this model remains a diluted Fe-solution model and shows some limitations for the description of some highly alloyed solutions.

That the reason why we chose to develop the Generalized Central Atom model (GCA) which unifies, in the same formalism, all these approaches, i.e., the Cell Model, the oxi-sulfides model and the Central Atom model. For the metallurgical slags, the benefits of this unification will come from a better description of the SRO than the one provided by the Cell model. For the liquid steel, the improvement will come also from the SRO description and from the fact that the GCA is not limited to diluted solutions in iron.

Description of the Structure

In the GCA model, the elements are distributed between two sublattices. The first one, constituted by the substitutional sites, is filled, in the case of the liquid steel, with metallic

elements whereas the other one, constituted by the interstitial sites, is filled with non-metallic elements. In the case of the metallurgical slags, the first sublattice is filled with the different cations and the second one with the different anions. Some interstitial sites could be left unoccupied in the case of the liquid steel, contrary to the metallurgical slags where all the sites are supposed to be occupied either by anions or by cations.

The liquid structure is described in terms of cells composed of a central atom and its shell of nearest neighbors. In a system with m components with t substitutional elements, the cell will be noted as:

$$\begin{matrix} i_1, i_2, \ldots i_k, \ldots i_t \\ J \\ j_{t+1}, \ldots j_r, \ldots j_m \end{matrix} \qquad \begin{matrix} \text{Atoms on substitutional sites} \\ \text{Central atom} \\ \text{Atoms on interstitial sites} \end{matrix}$$

In such a cell, around a central atom J that can be either substitutional or interstitial, there are i_1 atoms of element # 1, i_2 atoms of element # 2... located on substitutional sites, the total number of different elements being t. On the interstitial sites, there are j_{t+1} atoms of element # t+1, j_{t+2} atoms of elements # t+2... the total of elements on these sites being m-t. In the case of the metallic solutions, the index m can refer to the vacancies.
One of the main differences with the Central Atom model is that the number of nearest neighbors can depend on the nature of the central atom. This is the case, in particular, for the metallurgical slags. The number of nearest anions (and nearest cations) of a silicon atom is four whereas the number of nearest anions (and nearest cations) of a calcium atom is two. The total number of nearest neighbor atoms of an element i is denoted Z_i when these neighbors are placed on substitutional sites and z_i when they are placed on interstitial sites. For the liquid metallic phases, we chose a structure similar to the austenite. The number of substitutional sites is equal to the number of interstitial sites and the atoms have all the same number of neighbors. An atom i on a substitutional site has zi=6 neighbors located on interstitial sites and Z_i=12 on substitutional sites. Inversely, an atom j on an interstitial site has z_j=12 neighbors located on interstitial sites and Z_j=6 on substitutional sites. As an example, for liquid alloys Fe-Cr-Mn-Si-C-S, the substitutional sites are occupied by the solvent Fe as well as by the solutes Cr, Mn et Si. The interstitial sites are occupied by C and S, the other sites remain vacant. Thus, this solution can be represented by the formula (Fe, Cr, Mn, Si) (C, S,Va). For the metallurgical slags, the number of nearest anions of a given cation is equal to its valence state and is also the number of its nearest anions. For an anion O^{2-}, S^{2-} or $2F^{2-}$, the number of nearest cations is 2 and the number of its nearest anions is taken constant to Z=6 as it has been done for the oxi-sulfide model.

Parameters of the Model

Formation Energy Parameters

The energy of a cell is noted $\varphi^J_{\{i\}\{j\}}$ where J represents the central atom and {i} and {j} represent respectively the whole set of substitutional elements $i_1,\ldots,i_t$ and interstitial elements (including vacancies, if any) $j_{t+1},\ldots,j_m$. For the sake of simplicity, we suppose that this energy is the sum of the contributions of the two sites:

$$\varphi^J_{\{i\},\{j\}} = \varphi^J_{\{i\}} + \varphi^J_{\{j\}} \qquad (1)$$

In order to reduce the number of parameters, different assumptions have been formulated to describe the energy variation of the central atom according to the composition of chemical neighborhood. We chose the following expression in order to stay compatible with what had been previously taken for the cell model and for the central atom model:

$$\varphi^{J}_{\{i\}} = \sum_{k=1}^{t} i_k \varphi^{J}_{kk} + \frac{1}{2} \sum_{\substack{k,l=1 \\ k \neq l}}^{t} i_k i_l \varphi^{J}_{kl} \tag{2}$$

For the metallurgical slags, the parameters are inherited from the cell model where they are associated with the formation of an *asymmetric* cell from the two corresponding symmetric ones:

$$\tfrac{1}{2}\ k\text{-}J\text{-}k + \tfrac{1}{2}\ l\text{-}J\text{-}l \rightarrow k\text{-}J\text{-}l \tag{3}$$

Interaction Energy Parameters

Beside these formation energy parameters, interaction energy terms have been considered still to stay compatible with the Cell Model. The contribution of these terms to the Gibbs free energy has the following expression:

$$E = \frac{1}{2} RT \left(\sum_{J=1}^{m} \sum_{\{i\},\{j\}} N_J \, p^{J}_{\{i\}\{j\}} \ln Q^{J}_{\{i\}\{j\}} \right) \tag{4}$$

where N_J is the number of atoms J and $p^{j}_{\{i\}\{j\}}$ the probability to have the configuration {i} {j} around the atom J.

Some simple assumptions have been introduced for these interactions. First, as for formation energy parameters, an additive rule has been taken:

$$\ln Q^{J}_{\{i\}\{j\}} = \ln Q^{J}_{\{i\}} + \ln Q^{J}_{\{j\}} \tag{5}$$

Then, this interaction is assumed to vanish if all the atoms situated on this shell are not of the same nature:

$$\ln Q^{J}_{\{i\}} = \ln Q^{J}_{k} \neq 0 \text{ if and only if } i_k = Z_J \tag{6}$$

Finally, we have adopted for Q^{j}_{k} the following expression:

$$RT \ln Q^{J}_{k} = \frac{1}{2 N_R} \left(\sum_{i=1}^{t} Z_i N_i . E^{J}_{ki} + \sum_{j=t+1}^{m+1} Z_j N_j . E^{J}_{jk} \right) \text{ for } J > t \tag{7}$$

$$RT \ln Q^{J}_{l} = \frac{1}{2 N_S} \left(\sum_{j=t+1}^{m+1} z_j N_j . E^{J}_{lj} + \sum_{k=1}^{t} z_k N_k . E^{J}_{kl} \right) \text{ for } J \leq t \tag{8}$$

N_R and N_S are the number of atoms respectively on the interstitial and on the substitutional sites.

Gibbs Free Energy

The formalism to derive the expression of the various thermodynamic functions is similar to what had been proposed by Foo and Lupis [10, 11]. Prior to the calculation of the Gibbs free energy and of the chemical potentials, the partition function must be maximized. The corresponding equations are given in Table 1. They deliver the values of the Lagrange multipliers $\beta^{(J)}_k$. These equations are quite similar to the corresponding ones given by Foo and Lupis. Differences arise from the dependence of the number of neighbors on the nature of the central atom, from the expression of the formation energy and from the interaction energy parameters.

Table 1: Conditions of maximization of the partition function

Composition Variables		
n_{kl}: mole number of components $(C_l)_{u_l}(A_k)_{v_l}$		
$N_k = \sum_{l=t+1}^{m} v_l n_{lk} = V_k$	$1 \le k \le t$	(9)
$V_l = \sum_{k=1}^{t} v_l n_{lk}$	$t < l \le m$	(10)
$N_l = \sum_{k=1}^{t} u_l n_{lk}$	$t < l \le m$	(11)
$D_i = \sum_{l=i}^{m} V_l$ and $D = D_{t+1}$		(12)
Mass Balance Equations		
$\psi_k = \sum_{J=1}^{t} N_J \frac{P_k^J}{S^J} - Z_k N_k = 0$	$0 < k \le t$	(13)
$\psi_l = \sum_{J=1}^{t} N_J \frac{P_l^J}{s^J} - Z_l N_l = 0$	$t < l \le m$	(14)
$\psi'_k = \sum_{J=t+1}^{m+1} N_J \frac{P_k^J}{S^J} - z_k N_k = 0$	$0 < k \le t$	(15)
$\psi'_l = \sum_{J=t+1}^{m+1} N_J \frac{P_l^J}{s^J} - z_l N_l = 0$	$t < l \le m$	(16)
Expression of the Different Polynomials		
$p^J_{\{i\}} = \frac{Z_J!}{\prod_{k=1}^{t} i_k!} \exp\left(-\varphi^J_{\{i\}}\right) \prod_{k=1}^{t} \left(\frac{V_k}{D}\beta_k^{(J)}\right)^{i_k} \left(Q_k^J\right)^{9_{kJ}}$		and

$$p^{J}_{\{j\}} = \frac{z_J!}{\prod_{l=t+1}^{m+1} j_l!} \exp\left(-\varphi^{J}_{\{j\}}\right) \prod_{l=t+1}^{m+1} \left(\frac{V_l}{D}\beta_l^{(J)}\right)^{j_l} \left(Q_l^J\right)^{\vartheta_{lJ}} \tag{17}$$

$$S^J = \sum_{\{i\}} p^{J}_{\{i\}} \quad \text{and} \quad s^J = \sum_{\{j\}} p^{J}_{\{j\}} \tag{18}$$

$$P_k^J = \sum_{\substack{i_1,\ldots,i_t=0 \\ \sum_{k'} i_{k'}=Z_J}}^{Z_J} i_k p^{J}_{\{i\}} \quad \text{and} \quad P_l^J = \sum_{\substack{j_{t+1},\ldots,j_{m+1}=0 \\ \sum_{l'} j_{l'}=z_J}}^{z_J} j_l p^{J}_{\{j\}} \tag{19}$$

ϑ_{kJ} is equal to 1 if $i_k=Z_J$ and otherwise is equal to 0.
and $\{i\}=i_1,\ldots,i_t$ and $\{j\}=j_{t+1},\ldots,j_m$.

Note:

- The components of the liquid metallic phase are (Fe)(Va), (Si)(Va), (Fe)(C)...and those of the slags are $(Si)(O)_2$, $(Al)_2(O)_3$...
- When an exponent is put into brackets (as it is the case for $\beta_{(J)k}$), the value of the corresponding variables is the same for all elements in brackets as long as they belong to the same site. Thus the variables β have two sets of values (β_k, β_l) for $J \leq t$ and (β'_k, β'_l) for $J>t$.

The expression of the Gibbs free energy is given in Table 2. When compared to the central atom model [10], an additional term appears that comes from the normalizing factor of the expression of the mixing entropy (terms function of the D_i's). This term is inherited from the cell model and is, therefore, specific to the metallurgical slags. But it could also be adopted for the liquid metallic phase if, for example, it appears that, in such a phase, the number of nearest neighbors could differ from one element to the other.

The chemical potentials derived from the Gibbs free energy will have a much more complicated expression than in the Central Atom model. In particular, specific terms will appear resulting from the variations of the neighbors numbers as a function of the nature of the central atom and from the interaction energy.

Table 2: Expression of the Gibbs free energy

$$G/RT = -\sum_{l=t+1}^{m} \frac{u_l}{v_l}\left(D_l \ln\frac{D_l}{V_l} - D_{l+1}\ln\frac{D_{l+1}}{V_l}\right) + \sum_{k=1}^{t} N_k \ln\frac{V_k}{D} - \sum_{J=1}^{m+1} N_J \ln S^J s^J + \sum_{J=1}^{m+1}\left(Z_J \exp\beta_J + z_J \exp\beta'_J\right)\cdot N_J \tag{20}$$

First Applications to Liquid Steel

Since assessments on metallurgical slags are still in progress, up to now the main applications of the GCA model concern the liquid steel phase. They show the relevance of the chosen approach. The three examples given hereafter concern high-manganese steels. Figure 1 and Figure 2 show that the GCA model gives a satisfactory representation of the two phase diagrams whose description is of utmost importance for these grades: Fe-Mn-P and Fe-Mn-C.

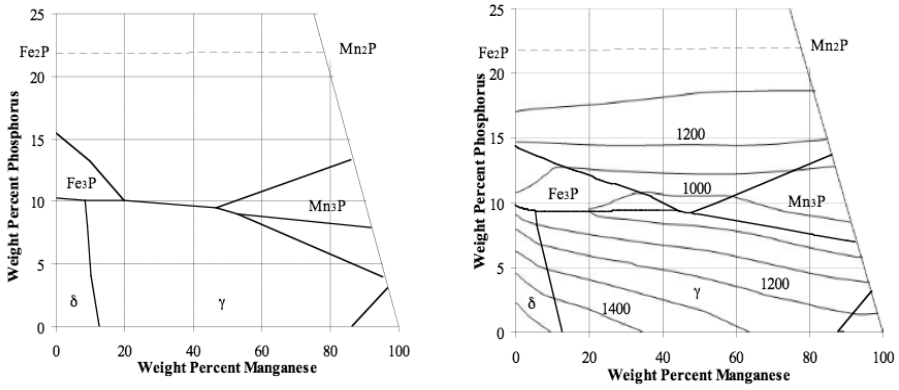

Figure 1: Comparison between the experimental Fe-Mn-P phase diagram (left) and the diagram calculated with the GCA model

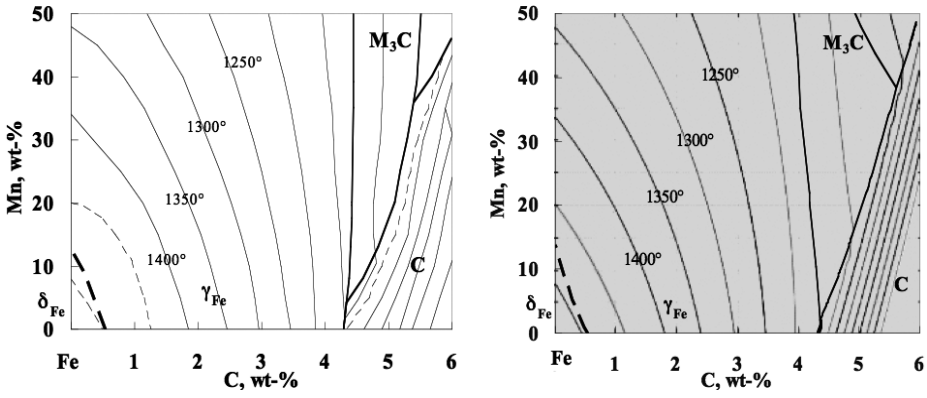

Figure 2: Comparison between the experimental C-Fe-Mn phase diagram (left) and the diagram calculated with the GCA model

Another illustration is given by Figure 3 which compares to the experimental data as they are reported in [12] the prediction of the model in terms of nitrogen solubility over the whole binary Fe-Mn. This prediction has been obtained without any ternary parameters. It is compared with the nitrogen contents as calculated with the sublattice model [13] which, for this system Fe-Mn-N, also does not contain any ternary term. The prediction of the GCA model appears to be better. This is believed to be due to a better description of the mixing entropy since (i) contrary to what is assumed by the sublattice model, in the GCA model, interstitial elements such as N, S, O are not distributed on the same sublattice as the substitutional elements Fe, Mn and (ii) the quasi-chemical approach permits to describe the SRO phenomenon.

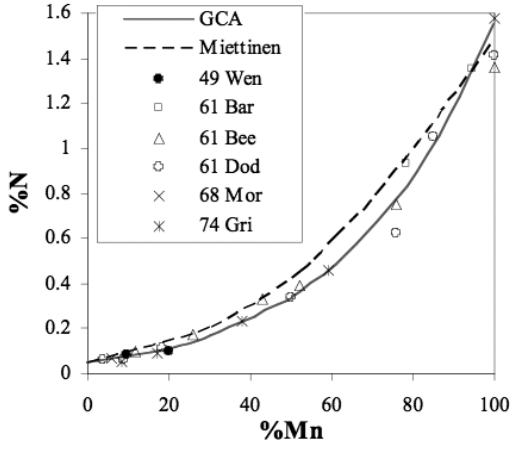

Figure 3: Nitrogen solubility under P_{N2} = 1 atm at 1550°C. C omparison between experimental data and calculations performed with the GCA and Miettinen models

KINETICS: THE PRECIPITATION MODEL MIPPHASOLACIDO

If equilibrium could be a reasonable approximation in a certain number of situations especially at high temperature, it is clear that a more realistic prediction can be obtained by kinetic simulations especially for precipitations occurring during steel solidification and at low temperatures in solid steel. Therefore, we have developed at ArcelorMittal Maizières a precipitation model, called *Mipphasolacido*, combining nucleation and mixed-controlled growth (i.e., controlled by mass transfer and/or interfacial kinetics) equations. The model beneficiates from the subroutines developed in Ceqcsi, a home-made chemical equilibrium calculation program, and, in particular, it can handle very different precipitates in terms of composition and stoichiometries. For instance, it has been initially developed to describe the precipitation of multicomponent liquid oxides during steel solidification [14], the thermodynamic properties of these oxides being described by the Cell Model.

Figure 4 gives a typical example of calculation performed by this program. The oxides under concern are liquid solutions of SiO_2-TiO_x-Al_2O_3–MnO precipitating during liquid steel cooling and solidification of a semi-killed steel (Al: 10 ppm, Ti: 110 ppm, O: 28 ppm). The figure gives the composition of the oxide *layer* growing on already existing particles according to their radii at a given time step. For small radii, growth is controlled by an interfacial reaction and the composition of the layer is constant up to radii around 0.01 μm. For large radii, growth is controlled by mass transfer and the composition of the layer is also constant but completely different from what it is for small inclusions, in particular the alumina content is much smaller. For inclusions with radii in between, the composition depends on their radii. The necessity to include the effect of an interfacial reaction in the model appeared clearly in experiments reported in [15] which showed an important impact of the steel sulfur content on TiN precipitation.

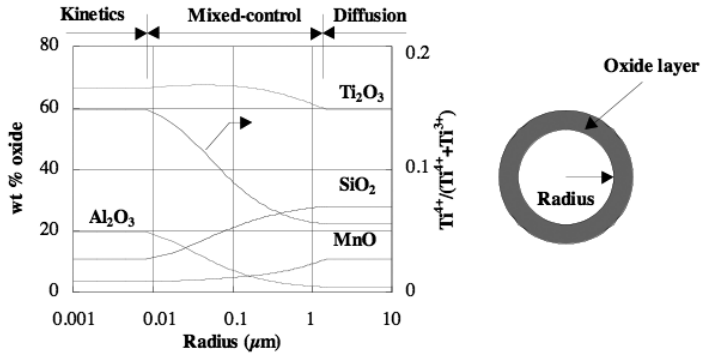

Figure 4: Composition of the new oxide layer precipitating on the existing precipitates as a function of their radius. The overall Ti-oxides content is expressed as wt % Ti_2O_3 but the proportion $Ti^{4+}/(Ti^{4+}+Ti^{3+})$ is also indicated

Mipphasolacido has been recently extended to the precipitation of multicomponent solid solutions with the possibility to take into account the competition between several precipitates.

Up to now, one of the weaknesses of the model was its cost in terms of computing times. That is why the direct quadrature method of moments (DQMOM), recently developed by Marchisio *et al.* [16], has been introduced to solve the population balances equations (PBE) which were formerly treated by a classical class method. The computation gain is coming from the fact that the growth rates have no more to be calculated for a large number of classes but only for a very limited number of *nodes*. First tests clearly show very promising results: the new method gives results very closed to the old one in terms of mean diameter, quantities and compositions of the precipitates but with computing times divided by a factor larger than 20, typically a few minutes instead of several hours.

THERMODYNAMICS AND FLUID DYNAMICS

Another important axis of research at ArcelorMittal Maizières concerns the modeling of the chemical reactions occurring in metallurgy vessels by coupling local reaction kinetics to fluid dynamics. A first stage consists in assuming local equilibrium and therefore to couple thermodynamics and fluid dynamics i.e., the CFD code Fluent™ and Ceqcsi. The example presented hereafter corresponds to the very first steps of a modeling of the desulfurization process in a secondary metallurgy ladle. Its main purpose was to develop all the subroutines necessary to tackle the full complexity of the problem.

In the example, desulfurization is performed by slag droplets (whose properties are described by the Cell Model) entrainment in the liquid steel flow at a rate of 5 kg/s in a 325 t vessel. Part of the particles is continuously trapped back by the slag layer. Figure 5 shows the evolution of the steel composition with time. In particular, we can see that the oxygen content goes through a minimum value. This rather complex behavior is the result of the reduction of the slag which tends to decrease the oxygen activity and of the desulfurization process which has the reverse effect since this reaction is an exchange of oxygen and sulfur between slag and metal:

$$CaO_{slag} + S \rightarrow CaS_{slag} + O \qquad (21)$$

As a consequence of the late oxygen content increase, Ca and Mg contents decrease during the second half of the simulation.

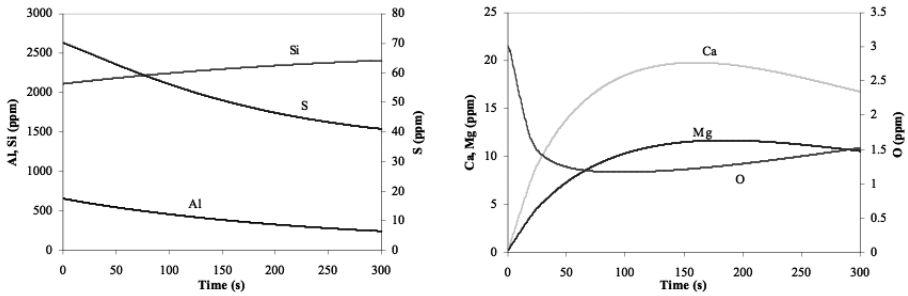

Figure 5: Evolution with time of the main elements contents in steel

CONCLUSIONS

The research conducted at ArcelorMittal Maizières in the domain of the physical-chemistry modeling is twofold. On the one hand, we want to improve our *elementary* models either in terms of accuracy as it is the case for the Cell Model or in terms of *computational efficiency* as its is the case for our kinetic model *Mipphasolacido*. And on the other hand, we want to take full profit of these advances to build complex combined models (thermodynamics + fluid dynamics or kinetics + fluid dynamics) which are necessary to get a realistic representation of the industrial processes. These models could then be used for instance in order to test any idea of improvements prior to trials in industrial conditions.

REFERENCES

Gaye, H. & Welfringer, J. (1984). *Modeling of the Thermodynamic Properties of Complex Metallurgical Slags*. Proc. of the 2nd International Symposium on Metallurgical Slags and Fluxes, Lake Tahoe, Edited by H.A. Fine and D.R. Gaskell, pp. 357-373. [1]

Guggenheim, E. A. (1952). *Mixtures*. Oxford, Clarendon Press. [2]

Gaye, H., Lehmann, J., Matsumiya, T. & Yamada, W. (1992). *A Statistical Thermodynamics Model of Slags: Applications to Systems containing S, F, P_2O_5 and Cr Oxides*. 4th International Conference on Molten Slags and Fluxes, Sendai, ISIJ, pp. 103-108. [3]

Lehmann, J., Gaye, H., Matsumiya, T. & Yamada, W. (1990). *A Statistical Thermodynamics Model of Sulphur and Fluorine bearing Iron and Steelmaking Slags*. 6th International Iron and Steel Congress, Nagoya ISIJ, pp. 256-263. [4]

Lehmann, J. & Gaye, H. (1999). T*hermodynamic Modeling of TiO_x-bearing Slags*. 82nd Steelmaking conference proceedings, Chicago, Iron and Steel Society, pp. 463-470. [5]

Gaye, H. & Lehmann, J. (1997). *Modelling of Slag Thermodynamic Properties*. From Oxides to Oxisulphides. Proc. 5th International Conference on Molten Slags, Fluxes and Salts, Sydney, Australia, ISS, pp. 27-34. [6]

Lupis, C. H. P. & Elliott, J. F. (1967). *Prediction of Enthalpy and Entropy Interaction Coefficients by the «Central Atoms» Theory*. Acta Met 15, pp. 265-274. [7]

Mathieu, J. C., Durand, F. & Bonnier, E. (1965). *L'atome entouré, entité de base d'un modèle quasi-chimique de solution binaire, I. Traitement général*. J. Chim. Phys., 62, p 1289. [8]

Pascal, B., Mathieu, J. C., Hicter, P., Desré, P. & Bonnier, E. (1971). *L'Atome Entouré, entité de Base d'un Modèle Quasi-chimique de Solution Binaire. VII*. Traitement Général d'une Solution Interstitielle. J. Chim. Phys. 68 p. 774. [9]

Foo, E-Hsin. & Lupis, C. H. P. (1973). *The Central Atoms Model of Multicomponent Interstitiel Solutions and its Applications to Carbon and Nitrogen in Ironalloys*. Acta Met. 21, pp. 1409-1430. [10]

Lupis, C. H. P. (1983). *Chemical Thermodynamics of Materials*. Elsevier Science Publishing Co., Inc. p. 482 [11]

Raghavan, V. (1987). P*hase Diagrams of Ternary Iron Alloys*. Part I. The Indian Institute of Metals. [12]

Miettinen, J. (1998). *Approximate Thermodynamic Solution Phase Data for Steels*. Calphad 22, pp. 275-300. [13]

Lehmann, J., Rocabois, P. & Gaye, H. (2001). Kinetic Model of Non Metallic Inclusions Precipitation during Steel Solidificatio. *Journal of Non-Crystalline Solids*, 282, pp. 61-71. [14]

Gaye, H., Rocabois, P., Lehmann, J. & Bobadilla, M. (1999). *Kinetics of Inclusion Precipitation during Steel Solidification*. Steel Research 70, pp. 356-361. [15]

Marchisio, D. L. & Fox, R. O. (2005). Solution of Population Balance Equations using the Direct Quadrature Method of Moments. *Journal of Aerosol Science*, 36, pp. 43-73. [16]